Bone Reports 19 (2023) 101705

Contents lists available at ScienceDirect

Bone Reports

journal homepage: www.elsevier.com/locate/bonr

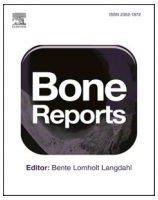

Effects of PTH on osteoblast bioenergetics in response to glucose

Victoria E. DeMambro [a,c], Li Tian [a,1], Vivin Karthik [c], Clifford J. Rosen [a,b,c], Anyonya R. Guntur [a,b,c,*]

[a] Center for Molecular Medicine, MaineHealth Institute for Research, Scarborough, ME, USA
[b] Tufts University School of Medicine, Tufts University, Boston, MA, USA
[c] Graduate School of Biomedical Sciences and Engineering, University of Maine, Orono, ME, USA

ARTICLE INFO

Keywords:
PTH bioenergetics
Glycolysis
Plasma Membrane Permeabilizer Assay
Agilent seahorse cellular flux analyzer

ABSTRACT

Parathyroid hormone acts through its receptor, PTHR1, expressed on osteoblasts, to control bone remodeling. Metabolic flexibility for energy generation has been demonstrated in several cell types dependent on substrate availability. Recent studies have identified a critical role for PTH in regulating glucose, fatty acid and amino acid metabolism thus stimulating both glycolysis and oxidative phosphorylation. Therefore, we postulated that PTH stimulates increased energetic output by osteoblasts either by increasing glycolysis or oxidative phosphorylation depending on substrate availability. To test this hypothesis, undifferentiated and differentiated MC3T3E1C4 calvarial pre-osteoblasts were treated with PTH to study osteoblast bioenergetics in the presence of exogenous glucose. Significant increases in glycolysis with acute ~1 h PTH treatment with minimal effects on oxidative phosphorylation in undifferentiated MC3T3E1C4 in the presence of exogenous glucose were observed. In differentiated cells, the increased glycolysis observed with acute PTH was completely blocked by pretreatment with a Glut1 inhibitor (BAY-876) resulting in a compensatory increase in oxidative phosphorylation. We then tested the effect of PTH on the function of complexes I and II of the mitochondrial electron transport chain in the absence of glycolysis. Utilizing a novel cell plasma membrane permeability mitochondrial (PMP) assay, in combination with complex I and II specific substrates, slight but significant increases in basal and maximal oxygen consumption rates with 24 h PTH treatment in undifferentiated MC3T3E1C4 cells were noted. Taken together, our data demonstrate for the first time that PTH stimulates both increases in glycolysis and the function of the electron transport chain, particularly complexes I and II, during high energy demands in osteoblasts.

1. Introduction

Bioenergetic pathways and metabolism of cells in the bone marrow including osteoblasts, osteocytes, bone marrow adipocytes and osteoclasts along with their corresponding progenitor cells are currently under intense investigation. Recent genetic deletion studies in mice utilizing Cre recombinase techniques have identified the importance of various metabolic pathways in regulating skeletal cell differentiation. Conditional deletion of genes in skeletal cells controlling substrate uptake, such as deletion of glucose transporter 1 (*Slc2a1*) in chondrocytes, osteoblasts and osteoclasts (Lee et al., 2018; Wei et al., 2015; Li et al., 2020) as well as the amino acid transporters sodium-dependent neutral amino acid transporter-2 (*Slc38a2*) and Alanine, Serine, Cysteine transporter 2 (*Slc1a5*) (Shen et al., 2022; Yu et al., 2019; Sharma et al., 2021) in osteoblasts, leads to abnormal bone homeostasis. Likewise, deletion of the fatty acid β-oxidation carnitine palmitoyltransferase-2 (*Cpt2a*) enzyme in osteoblasts (Kim et al., 2017) and osteoclasts (Kushwaha et al., 2022) also affected bone mass, further illuminating the importance of these bioenergetic pathways in controlling bone formation and remodeling.

Adenosine triphosphate (ATP) is generated in the cytoplasm through glycolysis (Glyc) and in the mitochondria through oxidative phosphorylation (OxPhos) as the two major energy sources. Metabolic reprogramming towards a particular ATP generating pathway has been identified in various cell types including immune T-cells, hematopoietic stem cells, and retinal ganglion cells (Buck et al., 2016; Simsek et al., 2010; Esteban-Martínez et al., 2017). This reprogramming functions not only to meet ATP demand but also to regulate various cellular functions

* Corresponding author at: MaineHealth Institute for Research, 81 Research Drive, Scarborough, ME 04074, USA.
E-mail address: Anyonya.Guntur@mainehealth.org (A.R. Guntur).
[1] Current address: Laboratory of Endocrinology and Metabolism, Department of Endocrinology, West China Hospital, Sichuan University, Chengdu, Sichuan, China.

https://doi.org/10.1016/j.bonr.2023.101705
Received 1 February 2023; Received in revised form 29 May 2023; Accepted 13 July 2023
Available online 24 July 2023

including maintenance of pluripotency, control of reactive oxygen species (ROS) production, autophagy, stress responses and signaling to various organelles like the endoplasmic reticulum to control protein synthesis (Graef and Nunnari, 2011; Finkel and Holbrook, 2000; Melber and Haynes, 2018). During bone formation, osteoblasts require high amounts of energy for secretion of collagen1α1 to form the extracellular matrix, which is then mineralized (Young et al., 1992). Mineralization also requires high amounts of energy as tissue-nonspecific alkaline phosphatase (TNAP) hydrolyzes ATP to fuel Ca2+ import into matrix vesicles secreted by osteoblasts for hydroxyapatite formation (Andrilli et al., 2023; Zhang et al., 2005; Favarin et al., 2020).

Different sources of precursor's cells that differentiate into osteoblasts have given rise to contrasting bioenergetic profiles. Studies utilizing primary bone marrow stromal cells (BMSCs) in vitro or osteoblasts using 2 photon microscopy ex vivo suggest there is a predominance of OxPhos at the differentiated stage for ATP generation (Shum et al., 2016; Schilling et al., 2022). While a recent contrasting report suggests that undifferentiated BMSCs primarily utilize OxPhos then increase their reliance on glycolysis as the differentiation process occurs (Misra et al., 2021). Likewise, other studies involving primary calvarial osteoblasts or the calvarial pre-osteoblast cell line, MC3T3E1C4 have revealed that the majority of ATP generated in the differentiated osteoblast is through glycolysis (Lee et al., 2020; Guntur et al., 2018). The Warburg effect (aerobic glycolysis) described in osteoblasts suggests that this preferential use of glycolysis in the presence of oxygen to generate ATP is coupled to mitochondria via Malic enzyme2 activity (Lee et al., 2020). In our previous work, we studied the energetic profiles of differentiating osteoblasts utilizing primary calvarial cells and calvarial pre-osteoblast cell lines with the XF Agilent Seahorse technology. Our data suggest that during differentiation, osteoblasts increase their glycolytic capacity for ATP production in response to exogenous glucose (Guntur et al., 2018). In this study, we set out to determine if the increases in oxidative phosphorylation observed in some pre-osteoblast cell types and conditions during differentiation were due to changes in mitochondrial electron transport chain complex activity. We used PTH a potent stimulus for osteoblast differentiation to study its effects on both bioenergetic pathways.

PTH is secreted by the parathyroid gland in response to low Ca^{+2} levels in circulation. Binding to its receptor, PTHR1, a G protein-coupled receptor (GPCR) predominantly expressed in osteoblasts, increases bone turnover, normalizing Ca^{+2} levels. The actions of PTH have been extensively studied and reviewed in the literature (Wein and Kronenberg, 2018; Rendina-Ruedy and Rosen, 2022). This hormone's role as an anabolic bone agent has been exploited by utilizing the FDA-approved drugs Teriparatide (PTH 1–34) or Abaloparatide (PTHrp) through intermittent administration to drive a net increase in bone mass. PTH is known to stimulate bone formation through direct signaling interactions with osteoblasts and osteocytes, which in turn express increased levels of receptor activator of nuclear factor-κB ligand (RANKL), a cytokine that stimulates osteoclastogenesis and activity (Fu et al., 2006). In addition, PTH signaling in the osteocyte decreases SOST activity, an inhibitor of WNT signaling increasing bone formation (Keller and Kneissel, 2005). Recently, studies have identified salt inducible kinases (SIKs) as being novel mediators of the effects of PTH on skeletal cells through their actions on class IIa histone deacetylases (HDAC4/5) and CREB regulated transcription coactivator 2(CRTC2) (Nishimori et al., 2019; Wein et al., 2016). Early studies of the role of PTH in inducing metabolic changes revealed increases in fatty acid oxidation and lactate generation in whole calvariae (Felix et al., 1978; Nichols and Neuman, 1987; Adamek et al., 1987). In support of these observations, recent work has shown that PTH treatment of primary calvarial cells or MC3T3E1 cells stimulates aerobic glycolysis and oxidative phosphorylation (Esen et al., 2015). In addition, PTH treatment of bone marrow adipocytes has been shown to prime them for lipolysis and the release of fatty acids, that are then taken up by osteoblasts and used as an additional fuel source (Maridas et al., 2019). In this study, we utilized the Agilent XF Seahorse technology to measure OCR and ECAR rates after PTH treatment before and after osteoblast differentiation in the presence or absence of exogenous glucose. We also utilized a novel cell permeabilized mitochondrial assay using pre and post differentiated osteoblasts lacking glycolytic function with and without PTH treatment to study the activities of complex I (CI) and II (CII) of the electron transport chain (ETC). These data provide insights into the effects of PTH on glycolysis and oxidative phosphorylation, which will be crucial for future studies targeting these bioenergetic pathways.

2. Materials and methods

2.1. Cell lines

For cellular assays performed on the XF 24: MC3T3E1C4 were purchased and obtained from ATCC (Manassas, VA) and cultured in growth media containing α-MEM (Gibco catalog # 112571 or A1049001) supplemented with 10 % v/v fetal bovine serum (FBS), 100 units/ml penicillin and 100 μg/ml streptomycin. Osteogenic differentiation was initiated by the addition of 8 mM β-glycerophosphate and 50 μg/ml ascorbic acid in growth media with media changes every other day for 7 days. Cells cultured in growth media were used as non-differentiating controls.

2.2. Reagents

Sigma (#P3671) for the XF24 assays, PTH was resuspended in 1 % acetic acid in H_2O, aliquoted, and frozen at −80 °C.

Bachem (#4011476) For the XF96 assays, PTH was hydrated in 4 mM HCL 1 % BSA and stored as above.

Seahorse XF Plasma Membrane Permeabilizer (PMP): Either a concentration of 1.5 nM (XF24) or 1 nM (XF96) of PMP (Agilent, #102504-100) was utilized according to manufacturer instructions.

2.3. Cell metabolism studies

2.3.1. Glycolytic and mitochondrial stress tests

2.3.1.1. XF24. MC3T3E1C4 cells were plated in a density of 50,000 cells/well in Seahorse XF24 V7 PS Cell Culture (Agilent # 100777-004) plates. All experiments were performed on the XF24 (Agilent) as described previously (Guntur et al., 2014, 2018). Briefly, cells were changed into XF DMEM media (Agilent # 103575-100) containing PTH or VEH (121 or 150 nM) with no additional exogenous substrates for 1 h before the start of the assay. A modified glycolytic stress test was then performed with sequential injections of 20 mM glucose (port A), 1 μM rotenone (port B), and finally, 50–100 mM 2-deoxy-D-glucose (2-DG; port C). In additional experiments with acute PTH treatment, port A was utilized to inject 121 nM PTH, and the subsequent compounds were injected as described above. Data were normalized to total μg of protein/well as measured by BioRad Protein assay reagent (# 500-0006). ATP production rates, glycolytic proton production rates (GlycoPPR), and mitochondrial proton production rates (MitoPPR) were calculated utilizing previously published methods (Guntur et al., 2018).

2.3.1.2. XF96. MC3T3E1C4 cells were plated at a density of 1500 cells/well in Seahorse XF96 V3 PS Cell Culture Microplates (101085-004) and cultured in ether growth or differentiation media for 7 days before being assayed. Briefly, cells were changed into XF DMEM with no additional exogenous substrates containing 150 nM PTH, 1 μM BAY876, Glut1 inhibitor (Sigma, #SML1774), or VEH for 1 h. A modified mitochondrial stress test was then performed through the sequential injection of glucose (20 mM, port A), oligomycin (2 μM, port B), FCCP (2 μM, port C), and antimycin A/rotenone (2 μM) in combination with Hoechst dye (20 μM, Port D). After the conclusion of the XF assay, cellular count/well

was measured on the Biotek Cytation I cellular imaging system (Agilent), and data was normalized utilizing the Seahorse XF Imaging and Cell Counting software (Agilent) (Guntur et al., 2018).

2.4. PMP assays

2.4.1. XF 24 based PMP assay

MC3T3E1C4 cells were plated as above. Cells were cultured in either growth (non-differentiated) or osteogenic differentiation media for 7 days. 3× Mitochondrial Assay Solution (MAS) was prepared according to the manufacturer's instructions. On the day of the assay, it was diluted to 1× MAS containing the final concentrations of mannitol 220 mM, 70 mM sucrose, KH_2PO_4 mM, 5 mM $MgCl_2$, HEPES 2 mM, EGTA 1 mM and 0.2 % Fatty Acid Free BSA. Cells were washed in 1× MAS and then changed over 180 μl of 1×MAS containing 4 mM ADP and 1.5 nM PMP in combination with 10 mM pyruvate, 0.5 mM malate to activate CI or 10 mM succinate and 2uM rotenone for CII (pH 7.4). Cells were then analyzed on the XF24 utilizing the following protocol: no equilibrium step, 2 cycles of Mix (.5 min), wait (.5 min), measure (2 min) for basal respiration readings and after each sequential injection of oligomycin (2 μM), FCCP (2 μM), rotenone and antimycin (2 μM). All injectables were diluted in 1× MAS with no BSA. For the PMP-XF24 assays no normalization was performed thus data are presented as the raw OCR values. Respiratory control ratios (RCR) were calculated by OCR rate after ADP stimulation/OCR rate after Oligomycin treatment (StateIII/StateIVo) (Salabei et al., 2014).

2.4.2. XF 96 based PMP assay

MC3T3E1C4 cells were plated as above and cultured in growth media for 7 days prior to being assayed. Cells were then treated with 150 nM PTH or VEH for 24 h or included in the 1× MAS solution immediately prior to the start of the assay. MAS and complex I and II solutions were prepared, and cells analyzed as above. In these studies cells were treated with oligomycin (1 μM), FCCP (3 μM) and Rotenone/Antimycin (2 μM) with Hoechst Dye (20 μM). Data were then normalized by cellular count/well as above.

2.5. Statistical analysis

Data were analyzed, and *p*-values were calculated using GraphPad Prism and a Student's *t*-test.

3. Results

3.1. Acute PTH treatment in undifferentiated MC3T3E1C4 results in increased glycolysis

We utilized the XF24 Seahorse analyzer and ran a modified glycolytic stress test to study the effects of PTH on glycolysis in undifferentiated MC3T3E1C4 cells. Cells grown overnight were then treated acutely with either PTH (121 nM) or Vehicle (VEH), and mitochondrial oxygen consumption rates (OCR) and glycolytic extracellular acidification rates (ECAR) were monitored for 100 min on the XF24. OCR and ECAR were relatively normal throughout the PTH treatment period (Fig. 1A) with no exogenous substrates. Upon glucose (20 mM) injection, there was a significant and immediate increase in ECAR in PTH treated cells (Fig. 1B). A further increase in ECAR with the addition of a complex I inhibitor rotenone was noted in both VEH and PTH treated cells, indicating that PTH treatment under these conditions does not drain glycolytic reserves completely. Treatment with 2-deoxyglucose (2-DG), an inhibitor of glycolysis, returned PTH treated ECAR rates to control levels confirming the rise in ECAR was due to changes in glycolysis. However, no changes were observed in OCR with PTH treatment with or without exogenous glucose present. To test the effects of a stronger concentration of PTH cells were then treated with 150 nM PTH which further confirmed the above observations (Fig. 1C & D). Proton production rates (PPR) and ATP production rates were then calculated. Analysis of PPR confirmed the increases in ECAR with PTH treatment in the presence of glucose were due to increased glycolysis (Fig. 1E). The observed increases in glycolysis in the presence of glucose with PTH treatment resulted in significantly higher glycoATP and totalATP production rates (Fig. 1F). A third series of experiments was then performed in which cells were pretreated with PTH (150 nM) or VEH for 60 min prior to being assayed on the XF24. No effects of acute PTH pretreatment were noted in basal OCR or ECAR (Fig. 1G & H). However, in these experiments upon addition of glucose (20 mM) a significant decrease in OCR was noted in PTH treated cells (Fig. 1F). This was coupled with a rapid and significant increase in ECAR suggesting a metabolic switch in substrate utilization for ATP generation with PTH treatment.

3.2. Acute PTH in differentiated MC3T3E1C4 cells results in increased glycolysis

Next, modified mitochondrial stress tests were performed on MC3T3E1C4 cells that had been differentiated in osteogenic media for 7 days on the XF96. Differentiated cells were pretreated with a combination of PTH (150 nM), a Glut1 inhibitor, BAY876 (1 μM) or VEH for 1 h prior to being assayed. No effects of PTH treatment were noted in either basal OCR or ECAR with or without GLUT1 inhibition (Fig. 2A & B). Upon addition of glucose a significant increase in ECAR with PTH treatment was observed compared to VEH (Fig. 2A) coupled with a non-significant trend for decreased OCR (Fig. 2B). The increased ECAR observed with combination of PTH and glucose treatment was significantly repressed upon GLUT1 inhibition (Fig. 2A). No significant differences in mitochondrial stress test parameters were noted between PTH and VEH treated differentiated cells except that there was a Crabtree effect (i.e. acute suppression of OCR with glucose addition) observed for the VEH and PTH differentiated cells confirming the increase seen with ECAR. Inhibition of GLUT1 in the presence of glucose increased basal OCR rates as well increased spare respiratory capacity, demonstrating the metabolic flexibility of differentiated MC3T3E1C4 cells (Fig. 2B).

3.3. Plasma membrane permeabilization (PMP) mitochondrial assays

The increase in glycolysis coupled with the lack of stimulation of oxidative phosphorylation observed with PTH treatment led us to ask if the ETC complex activity is normal in MC3T3E1C4 cells. We first set out to optimize the conditions of the assay. Utilizing a plasma membrane permeabilization (PMP assay), treatment with a bacterial toxin at a low concentration (1 nM) punctures the plasma membrane allowing the cytosolic constituents to leak out of the cell. Mitochondria are retained inside the cell and can be probed with various substrates and mitochondrial ETC inhibitors (oligomycin, FCCP and rotenone/antimycin) to test for activity. In combination with the PMP assay cells were treated with 1.5 nM PMP in combination with pyruvate/malate (10 mM/0.5 mM) to test Complex I or succinate/rotenone (10 mM/2 μM), to test Complex II activities (Fig. 3A). The non-differentiated cells showed a robust State II, basal respiration response with pyruvate/malate or succinate/rotenone as substrates. State III ADP-stimulated respiration (4 mM) was significantly higher in CII substrate treated cells versus CI. Oligomycin treatment (2 μM) revealed State IVo, respiration due to proton leak was higher in CII versus CI. Likewise, treatment with FCCP (2 μM) revealed State IIIu, maximal uncoupled-respiration, was higher in CII versus CI. Respiratory rate control ratios (RCR) were calculated and found to be ~3 in CI and CII (Fig. 3B) utilizing the PMP assay. Based on the above observations we conclude that CII has higher activity in undifferentiated MC3T3E1C4 osteoblast cells.

We next tested if there was a difference in ETC complex activity after differentiation in MC3T3E1C4 cells. We observed similar ETC complex activity in CI stimulated cells with CII exhibiting higher activity as in the non-differentiated cells. However, in CII stimulated cells, there was a

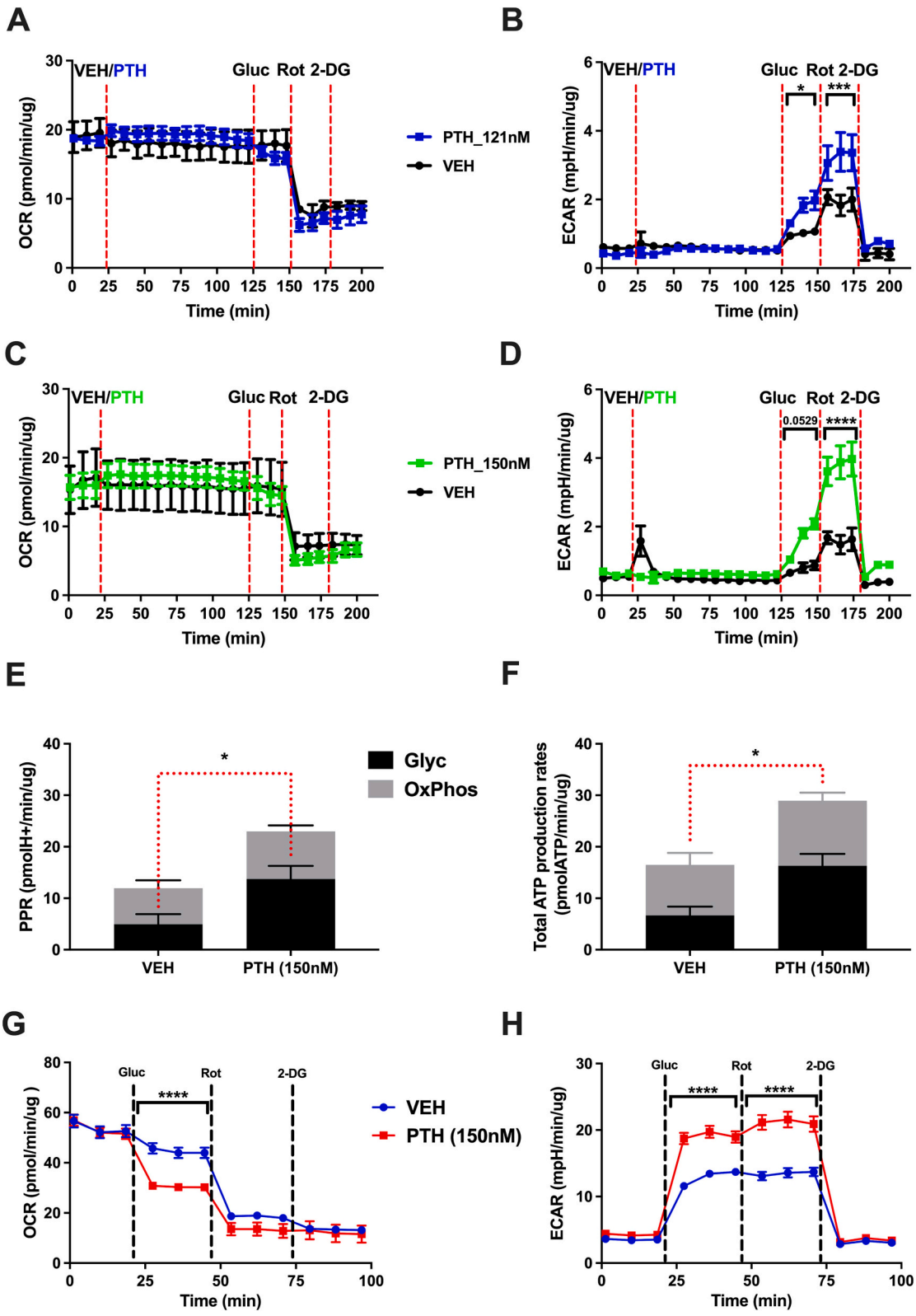

Fig. 1. Bioenergetic responses of undifferentiated MC3T3E1C4 cells to PTH treatment.
Modified glycolytic stress tests were performed utilizing the XF24 with sequential injections of VEH or PTH (121 nM or 150 nM; Port A), 20 mM glucose (Gluc; Port B), 1 μM rotenone (Rot; Port C) and 50 mM 2-DG (Port D). A) OCR and B) ECAR profiles for 121 nM PTH treatment studies. C) OCR and D) ECAR profiles for 150 nM PTH treatment studies. E) Proton production rates (PPR) from oxidative phosphorylation (OxPhos) and glycolysis (Glyc) for PTH 150 nM treatment experiments in the presence of glucose. F) ATP production rates from oxidative phosphorylation (OxPhos) and glycolysis (Glyc) for PTH 150 nM treatment experiments in the presence of glucose. G) OCR and H) ECAR profiles of undifferentiated MC3T3E1C4 treated with 150 nM PTH or VEH for 1 h prior to the start of the modified glycolytic stress test. All data were normalized to protein content/well, are presented as ±SEM and are the average of three independent experiments with a $n = 3–5$/treatment/experiment.

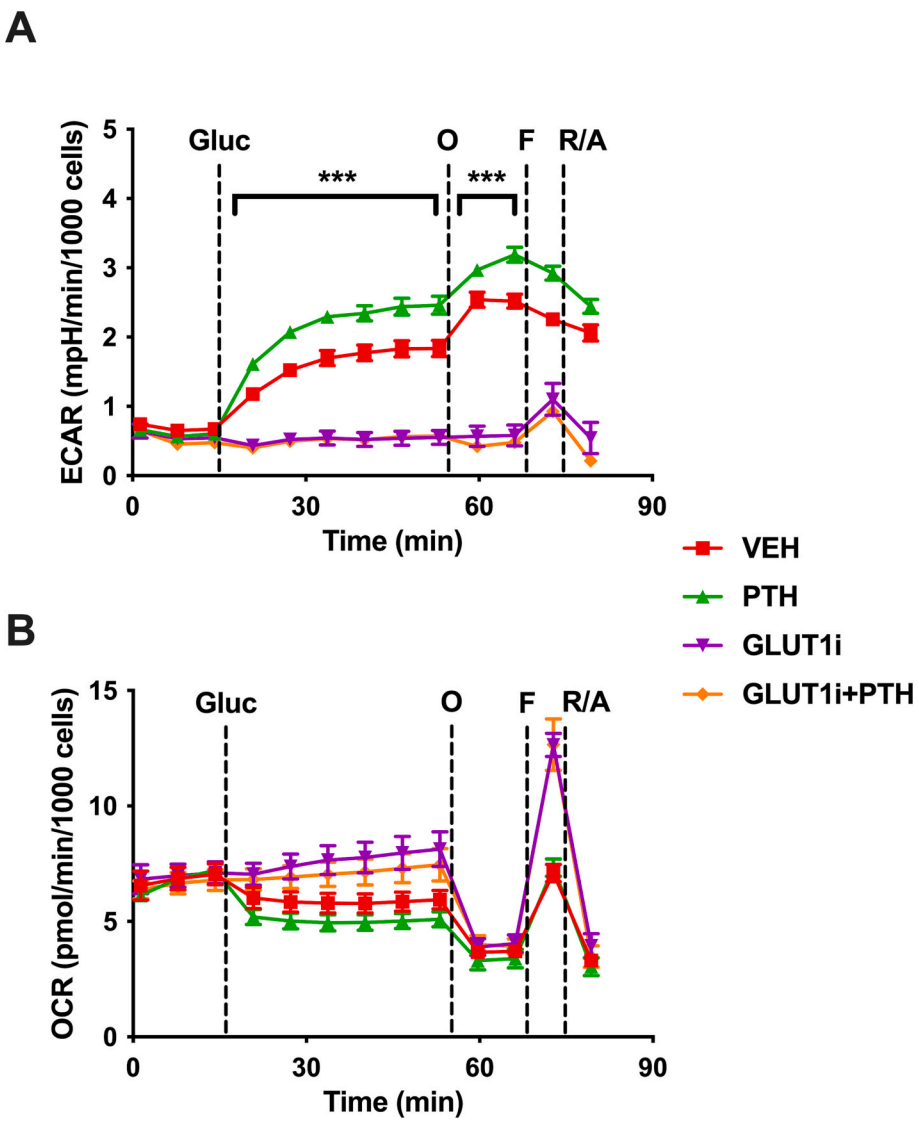

Fig. 2. Bioenergetic responses of differentiated MC3T3E1C4 cells to PTH treatment.
MC3T3E1C4 were differentiated for 7 days in osteogenic media and pretreated with 150 nM PTH or VEH for 1 h prior to being assayed on the XF96. A mitochondrial stress test was performed with sequential injections of 20 mM glucose (Gluc; Port A), 1 μM oligomycin (O, Port B), 1 μM FCCP (F, Port C) and 2 μM Rotenone/Antimycin/20 μM Hoechst dye (R/A/H; Port D). A) ECAR B) OCR profiles. All data are normalized to cell count/well and are presented as ±SEM. The data shown are representative of three independent XF96 experiments with n = 6–8/treatment/experiment.

complete lack of response to oligomycin, suggesting a loss of mitochondrial membrane integrity (Fig. 3C) with differentiation. State IIIu, increased with FCCP treatment, suggesting that there is still spare respiration capacity in differentiated cells despite the potential loss of membrane integrity. Analysis of RCRs revealed CI and CII values both <3 (Fig. 3D), suggesting that the PMP assay is unsuitable for assaying high functioning mitochondria in differentiated osteoblasts.

3.4. Effects of PTH treatment on CI and CII activity in undifferentiated MC3T3E1 cells

We next utilized the XF96 to test the effects of PTH treatment on CI and CII activity. To optimize the PMP concentration in undifferentiated MC3T3E1C4 cells on the XF96, PMP concentrations were titrated between 0.25 and 1.0 nm and treated with a combination of ADP (4 mM) and Complex II substrates (10 mM succinate/2 μM rotenone). At the lower PMP concentrations (0.25 and .50 nM) reduced State III respiration was noted coupled with a complete lack of response to FCCP suggesting incomplete permeabilization of the cell membrane at these concentrations. Cells treated with 0.75 or 1.0 nM responded appropriately to all drug treatments (Fig. 4A) with the 1.0 nM treatment resulting in the highest state III respiration. Calculated respiratory rate control ratios (RCR) revealed that the 1.0 nM treatment was optimal for MC3T3E1C4 cells (Fig. 4B). To identify the effects of PTH treatment on CI and CII activity undifferentiated MC3T3E1C4 cells were treated for either 24 h prior to or immediately with PTH (150 nM) or VEH before the start of the PMP assay. Immediate acute PTH treatment had no effects on either CI or CII activity (Fig. 4C & D). Treatment with PTH for 24 h resulted in a significant increase in State III ADP stimulated respiration compared to VEH in CI activated cells (Fig. 4E). All the other respiratory states were unchanged with PTH treatment and CI stimulation. Treatment with PTH for 24 h did not increase State III respiration with CII stimulation, nor was a significant effect noted in State IVo (Fig. 4F). However, upon treatment with FCCP, a significantly increased State IIIu respiration was observed suggesting PTH treatment increases the maximal capacity of undifferentiated MC3T3E1 cells in response to substrates oxidized through CII activity.

4. Discussion

In this study, we confirmed that PTH induces glycolysis acutely in the calvarial pre-osteoblast cell line MC3T3E1C4 in the presence of exogenous glucose. But importantly, using a novel PMP assay, we demonstrated that PTH can regulate the ETC through induction of CI and CII activity after longer treatments. ATP is required for up-regulation of collagen biosynthesis and ultimate mineralization in osteoblasts during

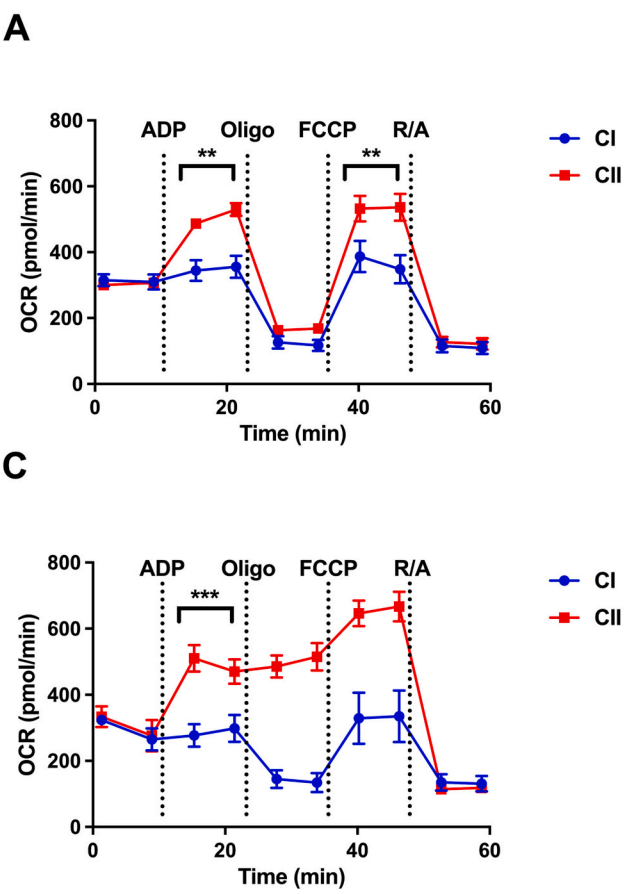

Fig. 3. Analysis of ETC complex I and II activities in permeabilized non-differentiated and differentiated MC3T3E1C4 cells.
MC3T3E1C4 cells were grown in either growth or osteogenic media for 21 days prior to being treated with PMP reagent (1.5 nM) in combination with either substrates for complex 1 (CI, blue) or (CII, red) and assayed on the XF24. Sequential injections included 4 mM ADP (Port A), 2 μM Oligomycin (Oligo; Port B), 2 μM FCCP (Port C) and 2 μM rotenone and antimycin (R/A; Port D). A) Undifferentiated MC3T3E1C4 OCR profile B) Respiratory control ratios for undifferentiated permeabilized cells. C) Differentiated MC3T3E1C4 OCR profile. D) Respiratory control ratio for differentiated permeabilized cells. RCR values were calculated by dividing State III ADP-stimulated respiration by State IVo, respiration due to proton leak. The data shown are representative of three independent XF96 experiments, presented as ±SEM with n = 3–5/treatment/experiment.

bone remodeling. Intermittent PTH drives those processes, by regulating osteoblast bioenergetics, although the substrates that fuel ATP generation have only recently been elucidated. For example, studies have shown that intact glucose and amino acid metabolism are required for anabolic PTH activity (Yamaguchi et al., 2005; Stegen et al., 2021). This likely occurs through PTH induction of IGF1 mediated signaling pathways (Esen et al., 2015). PTH treatment of MC3T3EC4 cells results in increased I*gf1* gene expression and the downstream activation of mTORC2 signaling increasing osteoblast differentiation. In addition, this study revealed an increase in oxidative phosphorylation with PTH treatment in MC3T3E1C4 osteoblasts, similar to what has been observed in other lineages, such as adipocytes (Larsson et al., 2016; Maridas et al., 2019). Furthermore, Esen et al., provided evidence that the majority of the increase in glucose uptake with PTH treatment is mediated through PKA signaling. Conversely, other studies in human SaOS-2 and rat osteoblast like UMR-106 cells have shown that the increased glycolysis with PTH (1–34) treatment is mostly mediated by PKC signaling, independent of cAMP/PKA and Na+/H+ exchanger pathways (Barrett et al., 1997; Belinsky et al., 1999; Belinsky and Tashjian Jr., 2000). Alternatively, another study using MC3T3E1C4 cells showed that PTH treatment enhanced osteoblast differentiation through GPR81-Gβγ-PLC-PKC-Akt signaling coupled with increased lactate production (Wu et al., 2018). In the current study, we utilized MC3T3E1C4 cells, in which we observed increased glycolysis with PTH treatment, although the response timing differs from published reports, most likely due to variations in the experimental protocol.

As seen in Fig. 1, there is an immediate increase in glycolysis and glycolytic ATP generation in response to acute PTH treatment in the presence of exogenous glucose. This observation is further strengthened by the increase in glycolysis with rotenone treatment that blocks CI of the ETC and results in the engagement of glycolytic reserves. This increase, in conjunction with the observations that PTH requires IRS1 signaling, glutamine metabolism and induces lipolysis in marrow adipocytes in the bone marrow suggests a general rewiring of metabolism in response to PTH. This allows the osteoblast to utilize all the available substrates immediately. However, the reliance on glycolysis is still maintained in the differentiated state, as seen in Fig. 2. GLUT1 is an insulin independent glucose transporter and has been implicated in skeletal biology as being one of the major regulators of glucose metabolism. We utilized a GLUT1 specific chemical inhibitor (GLUT1i) (Siebeneicher et al., 2016) to test the role of glucose uptake in this system. Inhibition of GLUT1 resulted in a complete loss in glycolysis, as seen in the ECAR trace for both the GLUT1i alone and GLUT1i + PTH. There is a concomitant increase in OCR (Fig. 2B) to compensate for the loss of glycolysis related ATP generation, and the cells presumably utilize internal endogenous sources of substrates.

There is also evidence that PTH treatment in osteoblasts can decrease mitochondrial respiration through a significant decrease in membrane potential resulting in reduced mitoATP generation (Troyan et al., 1997). We also observed a decrease in mitochondrial respiration with acute PTH treatment in the presence of glucose though only under certain conditions. This effect, similar to the Crabtree phenomenon (i.e. suppressed oxidative phosphorylation in response to glucose) (Guntur et al., 2018), was observed in cells that are differentiated presumably with high PTHR1 expression (Figs. 1G and 2B). The assays reported here were performed to study the activity of electron chain complexes during differentiation more closely by directly accessing CI and CII activity independent of glycolysis.

One major challenge to studying bone bioenergetics is the ability to isolate functional mitochondria from mineralized tissues. To overcome this challenge, we developed a permeabilization assay to test ETC activities. PMP was developed using a bacterial cytolysin (recombinant mutant perfringolysin O, rPFO) that forms ~250 Å pores at a low concentrations, resulting in perforation of the plasma membrane

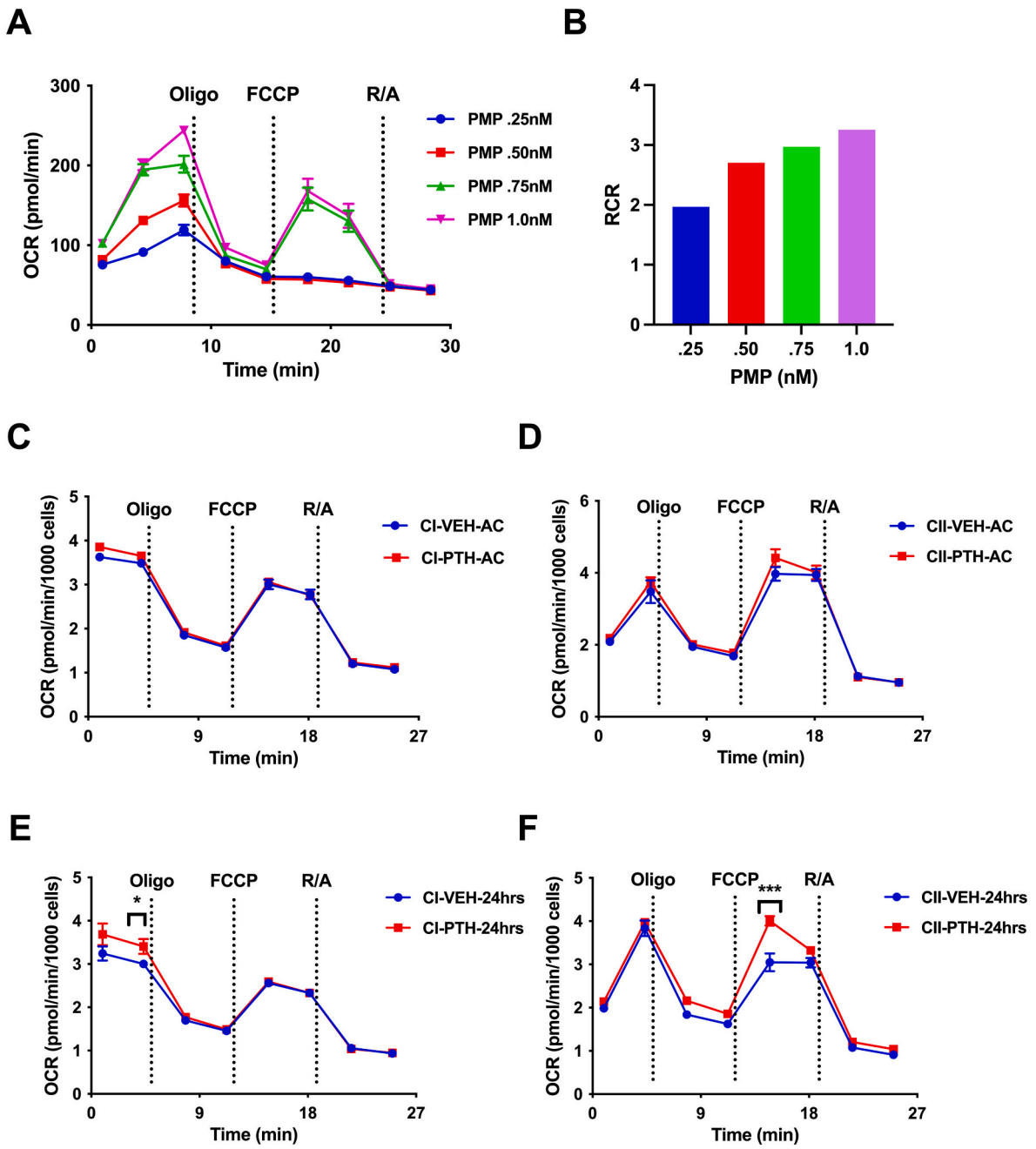

Fig. 4. Analysis of ETC complex I and II activities in permeabilized non-differentiated MC3T3E1C4 cells in response to acute or 24 h PTH treatment. MC3T3E1C4 cells were grown in growth media for 7 days prior to being treated with varying concentrations of PMP (0.25, 0.50, 0.75 or 1.0 nM) and a combination of 4 mM ADP and CII substrates to optimize the PMP concentration on the XF96. Sequential injections included 1 μM Oligomycin (Oligo; Port A), 3 μM FCCP (Port B) and 2 μM rotenone and antimycin (R/A; Port D). A) OCR profile and B) respiratory control ratios from PMP optimization assay. Cells were then grown as above and treated with PTH (150 nM) or VEH immediately before the assay in combination with PMP reagent (1 nM), 4 mM ADP and either substrates for complex 1 (CI) or (CII). C) CI stimulated activity in response to acute PTH treatment D) CII stimulated activity in response to acute PTH treatment. Cells were then treated with PTH or VEH for 24 h prior to being assayed. C) CI stimulated activity in response to 24 h PTH treatment D) CII stimulated activity in response to 24 h PTH treatment. The data shown are representative of three independent XF96 experiments and are presented as ±SEM with n = 3–5/treatment/experiment.

(Divakaruni et al., 2014). As a result, cytoplasmic contents within the cell are leaked out while double membraned organelles like the mitochondria, which also have a different cholesterol content than the plasma membrane, remain in the cell. These mitochondria in adherent monolayers can then be investigated in a manner similar to isolated mitochondria (Salabei et al., 2014). We used this technique to study CI and CII activities in response to specific substrates. CI substrates like pyruvate and glutamate in combination with malate to equilibrate with fumarate results in the generation of NADH. NADH can then transfer electrons through the ETC, reducing molecular oxygen to generate H_2O. The major component of CII (Succinate dehydrogenase) is a part of both the TCA cycle and ETC, addition of its substrate succinate results in the generation of FADH2, which then provides electrons to the ETC downstream. Co-treatment with rotenone inhibits complex 1 activity ensuring succinate stimulates complex II activity exclusively.

In the current study, this method was used on MC3T3E1C4 cells pre and post osteogenic differentiation. In non-differentiated cells, CII substrate, succinate resulted in higher OCR compared to CI substrate,

pyruvate. With differentiation we found that PMP treatment was not conducive for studying CII succinate-mediated respiration, as there was a loss in the response to oligomycin treatment, which was not attributable to increased proton leak. Uncoupling of the mitochondria, which would have resulted in maximal OCR in basal conditions, is also not the cause as we observed ADP induced OCR and further uncoupling upon FCCP treatment. We utilized two different treatments of PTH either 24 h or immediately before permeabilizing the cells and studying the OCR. The respiratory control ratio (RCR) for these cells and the conditions that we tested them under was ~3 for the undifferentiated cells and ~2.3 for CI and ~0.9 for CII stimulated differentiated cells. This is lower than what we have observed in prior studies with isolated mitochondria from mouse heart tissue (Beauchemin et al., 2020). The in vitro culture conditions of osteoblasts coupled with the increased mineralization of these cultures with differentiation, can potentially increase intercellular calcium levels and disrupt the mitochondrial membrane with PMP treatment. Thus, we conclude that this assay is more amenable for non-differentiated pre-osteoblastic cells. Future work will include studying the respiration activities linked to CIII and CIV in the presence or absence of PTH.

There are limitations to the current study. All the assays were done in MC3T3E1C4 cells; there is a need to check the PTHR1 receptor expression timing in these cells as we find some variability in the PTH response based on the passage number of the cells and how long they have been in culture. In vitro cell lines are known to drift in culture, thus in some cases, these cells might be refractory to PTH treatment or show the observed Crabtree effect. Using newer two photon microscopy techniques in vivo, primary bone marrow stromal cells or calvarial osteoblasts could provide other novel information. However, we propose generating and studying human iPSCs that can be differentiated into osteoblasts in a growth media that closely mimics human serum and physiological glucose levels (Cantor et al., 2017). This will allow for a physiologically relevant picture of osteoblast bioenergetics to be obtained. In this study, we utilized two different XF analyzers both the XF24 and XF96 both of which have different cell number and concentrations of reagents. An accompanying article in this special edition also points out a number of potential caveats (Sautchuk and Eliseev, 2022) to the use of isolated mitochondria and the use of XF analyzers the results in this manuscript can be utilized for developing and designing future studies.

5. Conclusions

In conclusion in this study, we treated MC3T3E1C4 calvarial pre-osteoblasts with PTH and observed significant increases in glycolysis in the presence of exogenous glucose with acute ~1 h PTH treatment with minimal effects on oxidative phosphorylation. This increased glycolysis was completely blocked by pretreatment with a Glut1 inhibitor (BAY-876) coupled with a compensatory increase in OxPhos. We have also developed a novel cell plasma membrane permeability mitochondrial (PMP) assay in MC3T3E1C4 cells in which glycolytic function is removed. In combination with CI and CII specific substrates, slight but significant increases in basal and maximal oxygen consumption rates with 24 h PTH treatment were observed. Taken together, our data demonstrate for the first time that PTH stimulates both increases in glycolysis and the function of the electron transport chain, particularly complexes I and II, during high energy demands in osteoblasts. This assay can be further employed to design studies to probe the effects of bone anabolic agents on the mitochondria. A recurring theme in the literature suggests that PTH's anabolic function requires intact glucose and amino acid metabolism. This study adds to this premise and suggests that PTH plays a role in priming the osteoblast to utilize any substrate available.

Declaration of competing interest

The authors declare that there is no conflict of interest.

Data availability

Data will be made available on request.

Acknowledgements

This work was supported by funds to GAR from NIH R03AR068095, NIH/NIGMS P20GM121301 and startup funds from Maine Health Institute for Research (MHIR). This work utilized services of the following core facilities at MHIR, Molecular Phenotyping Core, which is supported by NIH/NIGMS P30GM106391, the Physiology Core, supported by NIH/NIGMS P30GM106391 and P20GM121301. All cores also received support from the Northern New England Clinical and Translational Research Network NIH/NIGMS U54GM115516. The content is solely the responsibility of the authors and does not necessarily represent the official views of the National Institutes of Health.

References

Adamek, G., Felix, R., Guenther, H.L., Fleisch, H., 1987. Fatty acid oxidation in bone tissue and bone cells in culture. Characterization and hormonal influences. Biochem. J. 248, 129–137.

Andrilli, L.H.S., Sebinelli, H.G., Favarin, B.Z., Cruz, M.A.E., Ramos, A.P., Bolean, M., Millán, J.L., Bottini, M., Ciancaglini, P., 2023. NPP1 and TNAP hydrolyze ATP synergistically during biomineralization. Purinergic Signal 19, 353–366.

Barrett, M.G., Belinsky, G.S., Tashjian Jr., A.H., 1997. A new action of parathyroid hormone. Receptor-mediated stimulation of extracellular acidification in human osteoblast-like SaOS-2 cells. J. Biol. Chem. 272, 26346–26353.

Beauchemin, M., Geguchadze, R., Guntur, A.R., Nevola, K., Le, P.T., Barlow, D., Rue, M., Vary, C.P.H., Lary, C.W., Motyl, K.J., Houseknecht, K.L., 2020. Exploring mechanisms of increased cardiovascular disease risk with antipsychotic medications: risperidone alters the cardiac proteomic signature in mice. Pharmacol. Res. 152, 104589.

Belinsky, G.S., Tashjian Jr., A.H., 2000. Direct measurement of hormone-induced acidification in intact bone. J. Bone Miner. Res. 15, 550–556.

Belinsky, G.S., Morley, P., Whitfield, J.F., Tashjian Jr., A.H., 1999. Ca(2+) and extracellular acidification rate responses to parathyroid hormone fragments in rat ROS 17/2 and human SaOS-2 cells. Biochem. Biophys. Res. Commun. 266, 448–453.

Buck, Michael D., O'Sullivan, David, Klein Geltink, Ramon I., Curtis, Jonathan D., Chang, Chih-Hao, Sanin, David E., Qiu, Jing, Kretz, Oliver, Braas, Daniel, van der Windt, Gerritje J.W., Chen, Qiongyu, Huang, Stanley Ching-Cheng, O'Neill, Christina M., Edelson, Brian T., Pearce, Edward J., Sesaki, Hiromi, Huber, Tobias B., Rambold, Angelika S., Pearce, Erika L., 2016. Mitochondrial dynamics controls T cell fate through metabolic programming. Cell 166, 63–76.

Cantor, J.R., Abu-Remaileh, M., Kanarek, N., Freinkman, E., Gao, X., Louissaint Jr., A., Lewis, C.A., Sabatini, D.M., 2017. Physiologic medium rewires cellular metabolism and reveals uric acid as an endogenous inhibitor of UMP synthase. Cell 169 (258-72. e17).

Divakaruni, A.S., Rogers, G.W., Murphy, A.N., 2014. Measuring mitochondrial function in permeabilized cells using the seahorse XF analyzer or a clark-type oxygen electrode. Curr. Protoc. Toxicol. 60 (25.2.1-16).

Esen, Emel, Lee, Seung-Yon, Wice, Burton M., Long, Fanxin, 2015. PTH promotes bone anabolism by stimulating aerobic glycolysis via IGF signaling. J. Bone Miner. Res. 30, 1959–1968.

Esteban-Martínez, L., Sierra-Filardi, E., McGreal, R.S., Salazar-Roa, M., Mariño, G., Seco, E., Durand, S., Enot, D., Graña, O., Malumbres, M., Cvekl, A., Cuervo, A.M., Kroemer, G., Boya, P., 2017. Programmed mitophagy is essential for the glycolytic switch during cell differentiation. EMBO J. 36, 1688–1706.

Favarin, B.Z., Bolean, M., Ramos, A.P., Magrini, A., Rosato, N., Millán, J.L., Bottini, M., Costa-Filho, A.J., Ciancaglini, P., 2020. Lipid composition modulates ATP hydrolysis and calcium phosphate mineral propagation by TNAP-harboring proteoliposomes. Arch. Biochem. Biophys. 691, 108482.

Felix, R., Neuman, W.F., Fleisch, H., 1978. Aerobic glycolysis in bone: lactic acid production by rat calvaria cells in culture. Am. J. Phys. Cell Phys. 234, C51–C55.

Finkel, T., Holbrook, N.J., 2000. Oxidants, oxidative stress and the biology of ageing. Nature 408, 239–247.

Fu, Qiang, Manolagas, Stavros C., O'Brien, Charles A., 2006. Parathyroid hormone controls receptor activator of NF-κB ligand gene expression via a distant transcriptional enhancer. Mol. Cell. Biol. 26, 6453–6468.

Graef, M., Nunnari, J., 2011. Mitochondria regulate autophagy by conserved signalling pathways. EMBO J. 30, 2101–2114.

Guntur, Anyonya R., Le, Phuong T., Farber, Charles R., Rosen, Clifford J., 2014. Bioenergetics during calvarial osteoblast differentiation reflect strain differences in bone mass. Endocrinology 155, 1589–1595.

Guntur, Anyonya R., Gerencser, Akos A., Le, Phuong T., DeMambro, Victoria E., Bornstein, Sheila A., Mookerjee, Shona A., Maridas, David E., Clemmons, David E., Brand, Martin D., Rosen, Clifford J., 2018. Osteoblast-like MC3T3-E1 cells prefer glycolysis for ATP production but adipocyte-like 3T3-L1 cells prefer oxidative phosphorylation. J. Bone Miner. Res. 33, 1052–1065.

Keller, Hansjoerg, Kneissel, Michaela, 2005. SOST is a target gene for PTH in bone. Bone 37, 148–158.

Kim, S.P., Li, Z., Zoch, M.L., Frey, J.L., Bowman, C.E., Kushwaha, P., Ryan, K.A., Goh, B. C., Scafidi, S., Pickett, J.E., Faugere, M.C., Kershaw, E.E., Thorek, D.L.J., Clemens, T. L., Wolfgang, M.J., Riddle, R.C., 2017. Fatty acid oxidation by the osteoblast is required for normal bone acquisition in a sex- and diet-dependent manner. JCI Insight 2.

Kushwaha, P., Alekos, N.S., Kim, S.P., Li, Z., Wolfgang, M.J., Riddle, R.C., 2022. Mitochondrial fatty acid β-oxidation is important for normal osteoclast formation in growing female mice. Front. Physiol. 13, 997358.

Larsson, S., Jones, H.A., Göransson, O., Degerman, E., Holm, C., 2016. Parathyroid hormone induces adipocyte lipolysis via PKA-mediated phosphorylation of hormone-sensitive lipase. Cell. Signal. 28, 204–213.

Lee, S.Y., Abel, E.D., Long, F., 2018. Glucose metabolism induced by Bmp signaling is essential for murine skeletal development. Nat. Commun. 9, 4831.

Lee, W.C., Ji, X., Nissim, I., Long, F., 2020. Malic enzyme couples mitochondria with aerobic glycolysis in osteoblasts. Cell Rep. 32, 108108.

Li, B., Lee, W.C., Song, C., Ye, L., Abel, E.D., Long, F., 2020. Both aerobic glycolysis and mitochondrial respiration are required for osteoclast differentiation. FASEB J. 34, 11058–11067.

Maridas, David E., Rendina-Ruedy, Elizabeth, Helderman, Ron C., DeMambro, Victoria E., Brooks, Daniel, Guntur, Anyonya R., Lanske, Beate, Bouxsein, Mary L., Rosen, Clifford J., 2019. Progenitor recruitment and adipogenic lipolysis contribute to the anabolic actions of parathyroid hormone on the skeleton. FASEB J. 33, 2885–2898.

Melber, Andrew, Haynes, Cole M., 2018. UPRmt regulation and output: a stress response mediated by mitochondrial-nuclear communication. Cell Res. 28, 281–295.

Misra, B.B., Jayapalan, S., Richards, A.K., Helderman, R.C.M., Rendina-Ruedy, E., 2021. Untargeted metabolomics in primary murine bone marrow stromal cells reveals distinct profile throughout osteoblast differentiation. Metabolomics 17, 86.

Nichols, F.C., Neuman, W.F., 1987. Lactic acid production in mouse calvaria in vitro with and without parathyroid hormone stimulation: lack of acetazolamide effects. Bone 8, 105–109.

Nishimori, S., O'Meara, M.J., Castro, C.D., Noda, H., Cetinbas, M., da Silva Martins, J., Ayturk, U., Brooks, D.J., Bruce, M., Nagata, M., Ono, W., Janton, C.J., Bouxsein, M. L., Foretz, M., Berdeaux, R., Sadreyev, R.I., Gardella, T.J., Jüppner, H., Kronenberg, H.M., Wein, M.N., 2019. Salt-inducible kinases dictate parathyroid hormone 1 receptor action in bone development and remodeling. J. Clin. Invest. 129, 5187–5203.

Rendina-Ruedy, E., Rosen, C.J., 2022. Parathyroid hormone (PTH) regulation of metabolic homeostasis: an old dog teaches us new tricks. Mol. Metab. 60, 101480.

Salabei, J.K., Gibb, A.A., Hill, B.G., 2014. Comprehensive measurement of respiratory activity in permeabilized cells using extracellular flux analysis. Nat. Protoc. 9, 421–438.

Sautchuk, Rubens, Eliseev, Roman A., 2022. Cell energy metabolism and bone formation. Bone Rep. 16, 101594.

Schilling, K., Brown, E., Zhang, X., 2022. NAD(P)H autofluorescence lifetime imaging enables single cell analyses of cellular metabolism of osteoblasts in vitro and in vivo via two-photon microscopy. Bone 154, 116257.

Sharma, D., Yu, Y., Shen, L., Zhang, G.F., Karner, C.M., 2021. SLC1A5 provides glutamine and asparagine necessary for bone development in mice. Elife 10.

Shen, L., Yu, Y., Karner, C.M., 2022. SLC38A2 provides proline and alanine to regulate postnatal bone mass accrual in mice. Front. Physiol. 13, 992679.

Shum, L.C., White, N.S., Mills, B.N., Bentley, K.L., Eliseev, R.A., 2016. Energy metabolism in mesenchymal stem cells during osteogenic differentiation. Stem Cells Dev. 25, 114–122.

Siebeneicher, Holger, Cleve, Arwed, Rehwinkel, Hartmut, Neuhaus, Roland, Heisler, Iring, Müller, Thomas, Bauser, Marcus, Buchmann, Bernd, 2016. Identification and optimization of the first highly selective GLUT1 inhibitor BAY-876. ChemMedChem 11, 2261–2271.

Simsek, T., Kocabas, F., Zheng, J., Deberardinis, R.J., Mahmoud, A.I., Olson, E.N., Schneider, J.W., Zhang, C.C., Sadek, H.A., 2010. The distinct metabolic profile of hematopoietic stem cells reflects their location in a hypoxic niche. Cell Stem Cell 7, 380–390.

Stegen, S., Devignes, C.S., Torrekens, S., Van Looveren, R., Carmeliet, P., Carmeliet, G., 2021. Glutamine metabolism in osteoprogenitors is required for bone mass accrual and PTH-induced bone anabolism in male mice. J. Bone Miner. Res. 36, 604–616.

Troyan, M.B., Gilman, V.R., Gay, C.V., 1997. Mitochondrial membrane potential changes in osteoblasts treated with parathyroid hormone and estradiol. Exp. Cell Res. 233, 274–280.

Wei, J., Shimazu, J., Makinistoglu, M.P., Maurizi, A., Kajimura, D., Zong, H., Takarada, T., Lezaki, T., Pessin, J.E., Hinoi, E., Karsenty, G., 2015. Glucose uptake and Runx2 synergize to orchestrate osteoblast differentiation and bone formation. Cell 161, 1576–1591.

Wein, M.N., Kronenberg, H.M., 2018. Regulation of bone remodeling by parathyroid hormone. Cold Spring Harb. Perspect. Med. 8.

Wein, M.N., Liang, Y., Goransson, O., Sundberg, T.B., Wang, J., Williams, E.A., O'Meara, M.J., Govea, N., Beqo, B., Nishimori, S., Nagano, K., Brooks, D.J., Martins, J.S., Corbin, B., Anselmo, A., Sadreyev, R., Wu, J.Y., Sakamoto, K., Foretz, M., Xavier, R.J., Baron, R., Bouxsein, M.L., Gardella, T.J., Divieti-Pajevic, P., Gray, N.S., Kronenberg, H.M., 2016. SIKs control osteocyte responses to parathyroid hormone. Nat. Commun. 7, 13176.

Wu, Yu, Wang, Miaomiao, Zhang, Kefan, Li, Yingjiang, Manlin, Xu, Tang, Shaidi, Xiuxia, Qu, Li, Chunping, 2018. Lactate enhanced the effect of parathyroid hormone on osteoblast differentiation via GPR81-PKC-Akt signaling. Biochem. Biophys. Res. Commun. 503, 737–743.

Yamaguchi, M., Ogata, N., Shinoda, Y., Akune, T., Kamekura, S., Terauchi, Y., Kadowaki, T., Hoshi, K., Chung, U.I., Nakamura, K., Kawaguchi, H., 2005. Insulin receptor substrate-1 is required for bone anabolic function of parathyroid hormone in mice. Endocrinology 146, 2620–2628.

Young, M.F., Kerr, J.M., Ibaraki, K., Heegaard, A.M., Robey, P.G., 1992. Structure, expression, and regulation of the major noncollagenous matrix proteins of bone. Clin. Orthop. Relat. Res. 275–294.

Yu, Y., Newman, H., Shen, L., Sharma, D., Hu, G., Mirando, A.J., Zhang, H., Knudsen, E., Zhang, G.F., Hilton, M.J., Karner, C.M., 2019. Glutamine metabolism regulates proliferation and lineage allocation in skeletal stem cells. Cell Metab. 29 (966-78. e4).

Zhang, L., Balcerzak, M., Radisson, J., Thouverey, C., Pikula, S., Azzar, G., Buchet, R., 2005. Phosphodiesterase activity of alkaline phosphatase in ATP-initiated Ca(2+) and phosphate deposition in isolated chicken matrix vesicles. J. Biol. Chem. 280, 37289–37296.